




# A Chromosome-Length Reference Genome for the Endangered Pacific Pocket Mouse Reveals Recent Inbreeding in a Historically Large Population

Aryn P. Wilder <sup>1,\*</sup>, Olga Dudchenko<sup>2,3</sup>, Caitlin Curry<sup>1</sup>, Marisa Korody<sup>1</sup>, Sheela P. Turbek <sup>1,4</sup>, Mark Daly<sup>5</sup>, Ann Misuraca<sup>1</sup>, Gaojianyong Wang<sup>6</sup>, Ruqayya Khan<sup>2</sup>, David Weisz<sup>2</sup>, Julie Fronczek<sup>1</sup>, Erez Lieberman Aiden<sup>2,3,7,8,9</sup>, Marlys L. Houck<sup>1</sup>, Debra M. Shier<sup>1,10</sup>, Oliver A. Ryder <sup>1</sup>, and Cynthia C. Steiner<sup>1</sup>

<sup>1</sup>Conservation Science Wildlife Health, San Diego Zoo Wildlife Alliance, Escondido, CA, USA

<sup>2</sup>The Center for Genome Architecture, Department of Molecular and Human Genetics, Baylor College of Medicine, Houston, TX, USA

<sup>3</sup>Center for Theoretical Biological Physics and Department of Computer Science, Rice University, Houston, TX, USA

<sup>4</sup>Ecology and Evolutionary Biology, University of Colorado, Boulder, CO, USA

<sup>5</sup>Dovetail Genomics, Scotts Valley, CA, USA

<sup>6</sup>Department of Genome Regulation, Max Planck Institute for Molecular Genetics, Berlin, Germany

<sup>7</sup>UWA School of Agriculture and Environment, The University of Western Australia, Crawley, Australia

<sup>8</sup>Broad Institute of MIT and Harvard, Cambridge, MA, USA

<sup>9</sup>Shanghai Institute for Advanced Immunochemical Studies, ShanghaiTech, China

<sup>10</sup>Department of Ecology & Evolutionary Biology, University of California Los Angeles, Los Angeles, CA, USA

\*Corresponding author: E-mail: awilder@sdzwa.org.

Accepted: 21 July 2022

## Abstract

High-quality reference genomes are fundamental tools for understanding population history, and can provide estimates of genetic and demographic parameters relevant to the conservation of biodiversity. The federally endangered Pacific pocket mouse (PPM), which persists in three small, isolated populations in southern California, is a promising model for studying how demographic history shapes genetic diversity, and how diversity in turn may influence extinction risk. To facilitate these studies in PPM, we combined PacBio HiFi long reads with Omni-C and Hi-C data to generate a de novo genome assembly, and annotated the genome using RNAseq. The assembly comprised 28 chromosome-length scaffolds ( $N_{50} = 72.6$  MB) and the complete mitochondrial genome, and included a long heterochromatic region on chromosome 18 not represented in the previously available short-read assembly. Heterozygosity was highly variable across the genome of the reference individual, with 18% of windows falling in runs of homozygosity (ROH)  $> 1$  MB, and nearly 9% in tracts spanning  $> 5$  MB. Yet outside of ROH, heterozygosity was relatively high (0.0027), and historical  $N_e$  estimates were large. These patterns of genetic variation suggest recent inbreeding in a formerly large population. Currently the most contiguous assembly for a heteromyid rodent, this reference genome provides insight into the past and recent demographic history of the population, and will be a critical tool for management and future studies of outbreeding depression, inbreeding depression, and genetic load.

**Key words:** runs of homozygosity, effective population size, HiFi, chromosome conformation capture, mitochondrial genome.

## Significance

The design of optimal conservation strategies for the federally endangered Pacific pocket mouse, a subspecies that has undergone substantial declines and is under intensive management, relies on precise estimates of genome-wide heterozygosity, inbreeding, demographic history, and chromosomal variation. We generated a chromosome-length reference genome for this species, and found massive stretches of homozygosity across a genome with relatively high baseline heterozygosity, reflecting inbreeding in a formerly large population. The high degree of contiguity of this reference genome enabled the detection of signatures of contemporary inbreeding, highlighting the value of high-quality reference genomes for the management of endangered species, and conservation of biodiversity.

## Introduction

Chromosome-length reference genomes are fundamental tools for addressing questions in biology, from evolutionary innovation to the underpinnings of disease (Rhie *et al.* 2021; Blaxter *et al.* 2022). Highly contiguous assemblies provide a more complete understanding of historical and contemporary diversity and demographics, and can enable the precise estimation of parameters relevant for the study, management, and conservation of endangered species (Robinson *et al.* 2021; Totikov *et al.* 2021).

The federally endangered Pacific pocket mouse (PPM; *Perognathus longimembris pacificus*) is a valuable model species for studying the interplay between genetic variation and extinction risk. Having been extirpated from most of its distribution along coastal southern California in the 1930s (Brylski *et al.* 1998; King *et al.* 2022), the subspecies persists in three small, isolated populations in Orange and San Diego counties with very low effective population sizes ( $N_e = 3.3$ , 25.0, and 50.6; Swee *et al.* 2003; Wilder *et al.* 2020). It is the target of intensive conservation measures involving both in situ management of wild populations and an ex situ breeding program for reintroduction (Brylski *et al.* 1998; King *et al.* 2022). Microsatellite and mitochondrial markers have provided estimates of population differentiation, diversity,  $N_e$ , and relatedness, but genomic data would give additional resolution needed to address remaining questions relevant to population management. For example, a fitness analysis suggested that inbreeding and genetic load may play a role in limiting reproductive success (Wilder *et al.* 2020), and evidence of karyotype variation within *P. longimembris* (Patton 1967; McKnight and Lee 1992) and within PPM (King *et al.* 2020) has raised concerns that outbreeding depression could constrain fitness when populations are crossed. The use of genomic data to address these questions has been hindered by the lack of a highly contiguous reference genome. A draft genome for PPM, generated as part of a multispecies alignment of 241 mammalian genomes, was previously assembled from short-read sequence data using DISCOVAR (Zoonomia Consortium 2020). However, this genome was too fragmented (scaffold N50 < 25 KB) and incomplete (71.7% complete BUSCO genes; table 1) to study structural

variation that may contribute to outbreeding depression, or to estimate long runs of homozygosity (ROH) to infer inbreeding coefficients.

Here, we combined PacBio HiFi long reads with both Dovetail Omni-C and Hi-C data to assemble a reference genome with chromosome-length scaffolds and a complete mitochondrial genome. We then mapped short-read data to the genome to estimate demographic history, heterozygosity, and ROH across the genome of the reference individual.

## Results and Discussion

### De Novo Genome Assembly

The final genome assembly comprised 6,180 scaffolds (scaffold N50 = 72.68 MB), including 28 chromosome-length scaffolds (fig. 1; table 1). The number of chromosome-length scaffolds is in agreement with the inferred ancestral karyotype for *P. longimembris* ( $2n = 56$ ; McKnight 1995). The anchored scaffold length comprises 89.6% of the total genome length (1,922,316,746 bp of

**Table 1**

Genome Assembly Statistics Comparing the Final Assembly (HiFi + Omni-C + Hi-C) to the Previous DISCOVAR Assembly

	Final Assembly	DISCOVAR Assembly
Number of scaffolds	6,180	2,409,818
Total size of scaffolds	2,212,099,196	2,601,695,796
Longest scaffold	163,161,067	625,731
N50 scaffold length	72,679,016	24,714
L50 scaffold count	11	23,202
N50 contig length	7,389,774	17,686
L50 contig count	73	34,664
GC content	41.98%	41.84%
Complete BUSCOs	246 (96.4%)	183 (71.7%)
Complete & Single-Copy BUSCOs	239 (93.7%)	175 (68.6%)
Complete & Duplicated BUSCOs	7 (2.7%)	8 (3.1%)
Fragmented BUSCOs	3 (1.2%)	46 (18.0%)
Missing BUSCOs	6 (2.4%)	26 (10.3%)

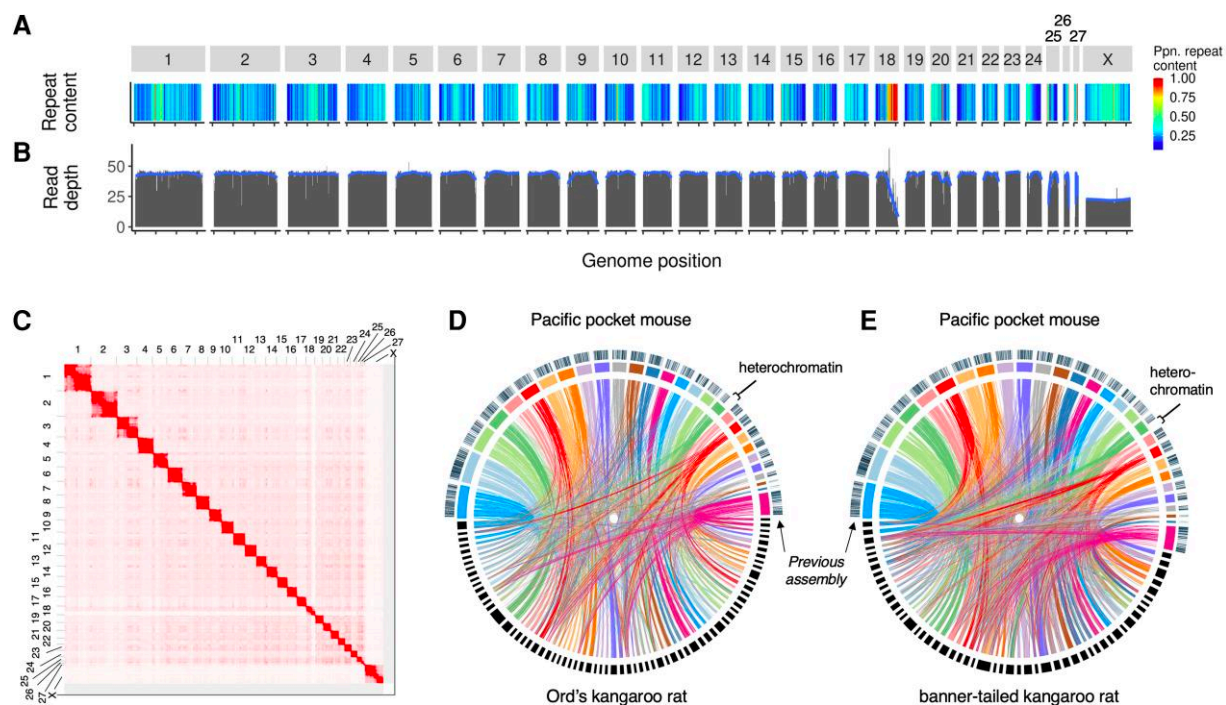


**FIG. 1.**—Chromosome-length scaffolds of the PPM genome assembled from HiFi, Omni-C, and Hi-C data. (A) Repeat content in 500 KB windows. Warmer colors show higher repeat content. (B) Mapping depth of short reads from the same individual. (C) Heatmap showing, on the scale from white to red, the frequency of 3D contact between any two loci of the PPM genome as measured by Hi-C sequencing. The same Hi-C data were used for scaffolding the genome to chromosome-length. Twenty-eight squares along the diagonal represent chromosome territories. An interactive version of this figure is available at <https://tinyurl.com/25vywofz> (Robinson *et al.* 2018). (D and E) Synteny between the PPM genome and two kangaroo rats, *D. ordii* (D) and *D. spectabilis* (E). Chromosome-length scaffolds of the PPM genome are colored, and scaffolds/contigs of the kangaroo rat genomes are black. Lines between the genomes show alignments >500 bp. Bars above the PPM scaffolds show the location of scaffolds >100 KB from the previous PPM genome assembly. The heterochromatic region of chromosome 18, absent from the larger scaffolds of the previous assembly, is highlighted.

2,212,099,196 bp total), that is ~290 Mb remain unanchored. Of this, ~20 Mb are identifiable as Y-chromosome-related (based on elevated contact frequency with pseudoautosomal regions of the X-chromosome). The rest appears to be hard-to-assemble, repeat-rich heterochromatin, and centromeric repeats. The total assembly length of 2.21 GB was smaller than that of the previous draft DISCOVAR assembly (2.60 GB). Genome size estimated from kmers of publicly available short-read data generated for the draft assembly (SRR11431899) ranged from 1.86 to 1.94 GB (supplementary fig. S3 and table S6, Supplementary Material online), which is closer to the size of our assembly. The assembly had 96.4% complete BUSCO genes in the Eukaryota database (eukaryota\_odb10), and 92.3% complete BUSCO genes in the Glires database (glires\_odb10). The gene annotation for the nuclear genome had 93.5% complete genes in the glires\_odb10 BUSCO database, with 0.6% fragmented genes and 2.6% missing genes. The complete mitochondrial genome was 16,293 bp (38.6% GC content), and included the control region, 22 tRNA genes, 2 ribosomal RNA genes, and

13 protein-coding genes (supplementary fig. S2 and table S3, Supplementary Material online).

Using RepeatMasker (Smit 2004), 41% of the genome was classified as repetitive, largely in the form of short- and long-interspersed nuclear elements and long terminal repeats (supplementary table S5, Supplementary Material online). Using de novo repeat identification (Girgis 2015), 29.6% of the genome was repetitive, including a >20 MB span of chromosome 18 (fig. 1A). This heterochromatic region was not represented among the larger contigs (>100 KB) of the DISCOVAR assembly (fig. 1D and E), and short-read data mapped to the genome had markedly lower depth in this region (fig. 1B), highlighting the difficulty of assembling and mapping highly repetitive regions with short reads.

We evaluated genome-wide synteny between PPM and two heteromyid species, Ord's kangaroo rat (*Dipodomys ordii*) and banner-tailed kangaroo rat (*D. spectabilis*; Harder *et al.* 2022, fig. 1D and E). Although not closely related to PPM (22.3 Myr to the most recent common ancestor; Hafner *et al.* 2007), they are the closest species with contiguous reference genomes (scaffold N50 = 11.9 MB

and contig N50 = 9.6 MB for *D. ordii* and *D. spectabilis*, respectively). Frequent rearrangements between genomes, as demonstrated by contigs in the *Dipodomys* genomes that map to multiple PPM chromosomes and vice versa, is consistent with high cytogenetic variability across rodents (Romanenko and Volobouev 2012; Zhou et al. 2020).

### Genome-Wide Heterozygosity and Demographic History

The distribution of genetic diversity was highly variable across the genome. Heterozygosity was consistently elevated near telomeres, and heterozygous regions were interspersed with large spans of homozygosity. Mean autosomal heterozygosity was relatively high ( $2.00 \times 10^{-3}$ , ~2 variants per KB), but 25.9% of autosomal 50 KB windows had virtually no heterozygosity (i.e., levels similar to those on the single-copy X chromosome) (fig. 2A). Nearly half (48.1%) of homozygous windows were part of ROH >5 MB in length, including a ~67.1 MB span of chromosome 2 (fig. 2A and B). These long ROH likely stem from inbreeding within the last ten generations (fig. 2B), assuming 100 MB identity-by-descent tracts are inherited per meiosis (Thompson 2013; van der Valk et al. 2019). ROH are more common in regions of low recombination, for example on the X chromosome or within structural variants, but very long ROH are more likely to be caused by recent inbreeding (Ceballos et al. 2018).

In contrast with these signatures of contemporary inbreeding, Pairwise Sequentially Markovian Coalescent (PSMC) estimates suggest large historical effective population sizes for PPM.  $N_e$  decreased between 150 and 100 Ka from ~400,000 to ~50,000, where it remained up to 10 Ka (fig. 2C). Selective sweeps, which are common in large populations, can also produce signals that appear as population contraction by PSMC (Schridder et al. 2016). The timing of the inferred historical population contraction coincides with the beginning of the last glacial period, a period of diversification, and speciation for many taxa in southern California (Vandergast et al. 2008), likely including *P. longimembris*, which consists of 16 recognized subspecies ([www.itis.gov](http://www.itis.gov); accessed 13 December 2021). Other heteromyids show similar fluctuations and large historical  $N_e$ , including the federally endangered Stephen's kangaroo rat (*Dipodomys stephensi*; Harder et al. 2022). The large historical  $N_e$  inferred from PSMC is supported by the relatively high heterozygosity outside of ROH windows (mean =  $2.70 \times 10^{-3}$ ).

The large historical  $N_e$  stands in contrast with signatures of recent inbreeding in the reference individual. The ROH-based inbreeding coefficient,  $F_{\text{ROH} > 1\text{MB}} = 0.18$ , is on par with iconic endangered species such as South Asian tigers (*Panthera tigris*; Armstrong et al. 2021), some Iberian lynx (*Lynx pardinus*) populations (Abascal et al. 2016), Malayan pangolins (*Manis javanica*; Hu et al. 2020), and

pygmy hogs (*Porcula salvania*; Liu et al. 2021). However, inbreeding can occur even when populations are large, especially for some heteromyid rodents with small natal dispersal distances (Waser et al. 2006), and thus inbreeding levels may vary across individuals. Heterozygosity at 15 previously published microsatellite loci suggests the reference individual was more inbred than its population, the largest of the three extant PPM populations (Spencer 2005). Heterozygosity was lower in the reference individual (proportion of heterozygous loci  $pHt = 0.47$ ) than the population average (mean  $pHt = 0.70$ ,  $n = 14$ ; data from Wilder et al. 2020), but was not markedly different from PPM range-wide (mean  $pHt = 0.53$ ,  $n = 35$ ), including populations that have experienced the largest declines. Additional genomic samples are needed to estimate the level of inbreeding across the subspecies.

Habitat fragmentation from urbanization has led to population declines in this and other species across southern California (Bolger et al. 1997). Formerly large populations that recently contracted may be at increased risk of inbreeding depression from recessive deleterious variants, which may hinder recovery and exacerbate the threat of extinction (Hedrick and Garcia-Dorado 2016). This high-quality reference genome provides a critical tool for current and future studies of inbreeding depression, genetic load, structural variation, and outbreeding depression with population genomic data in this subspecies, and demonstrates the value of highly contiguous assemblies for the management and conservation of biodiversity.

## Materials and Methods

We provide an overview of the methods below. Further details can be found in the [supplementary materials](#), [Supplementary Material](#) online.

### Sample Collection, DNA Extraction, and Library Preparation

A wild-born male PPM was collected in 2012 from Santa Margarita (San Diego, CA, USA), the largest and most genetically diverse extant population (Swei et al. 2003; Wilder et al. 2020). The individual was a founder for the PPM Conservation Breeding Program at the San Diego Zoo Wildlife Alliance (Shier 2014). A fibroblast cell line was established after the death of the individual in 2019 (King et al. 2020). Cells were harvested at passage 6 (for Omni-C data generated here and short-read data generated previously) and passage 11 (for RNAseq, HiFi, and Hi-C), cryopreserved and stored at  $-8^{\circ}\text{C}$ .

### De Novo Genome Assembly

High molecular weight DNA was extracted from ~20 M fibroblasts, and a Sequel HiFi Library was prepared and

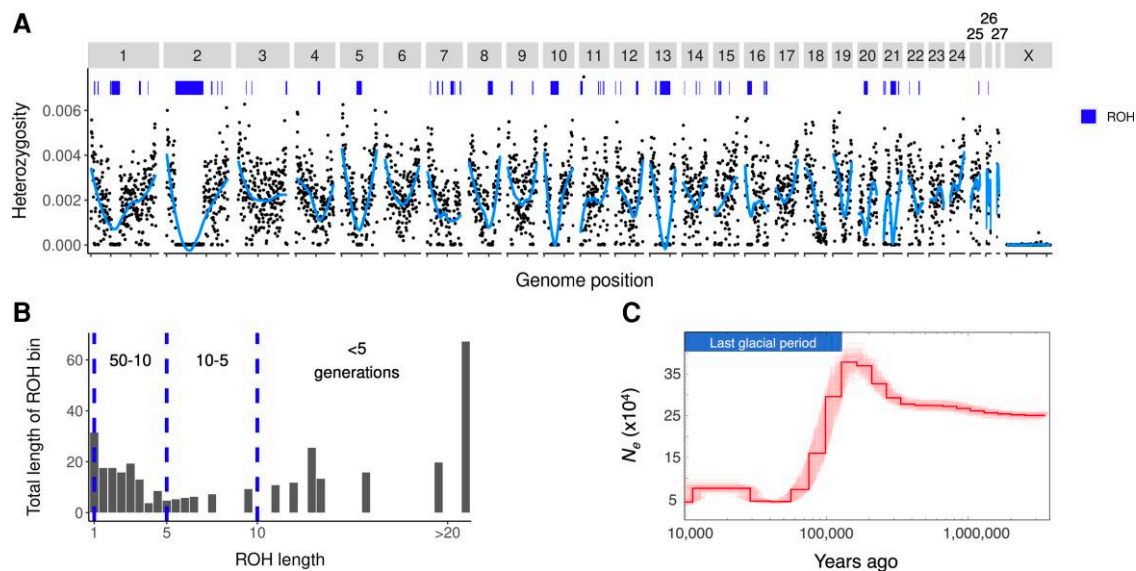


**Fig. 2.**—The distribution of heterozygosity across the PPM genome reflects recent inbreeding. (A) Mean heterozygosity in 500 KB windows (points), sliding mean heterozygosity (lines), and runs of homozygosity (ROH > 1 MB; bars at top). (B) Total lengths of ROH in each 1 MB bin (for 1 MB < ROH < 67 MB). Hatched lines and corresponding labels show the approximate number of generations since inbreeding for ROH of a given size range, assuming 100 MB tracts are inherited per meiosis. (C)  $N_e$  over time, showing population decline at the beginning of the last glacial period followed by stable  $N_e \sim 50,000$ . Lighter lines are replicate PSMC runs, and the dark line shows the mean of all replicates.

sequenced with two SMRT cells (Pacific Biosciences) using the Sequel II Sequencing Kit v2.0. We used the Peregrine assembler (Chin and Khalak) for the de novo assembly of 51.2 GB of HiFi reads with quality scores  $Q > 20$  (23.3× genome coverage).

For the Dovetail Omni-C library, chromatin from  $\sim 10.5$  M fibroblasts was fixed in place with formaldehyde, extracted, and digested with DNase I. Chromatin ends were repaired, adapter-containing ends were ligated by proximity ligation, crosslinks were reversed, and the DNA purified. Libraries were sequenced to  $\sim 30\times$  coverage. The HiFi-based draft and Omni-C library reads with  $MQ > 50$  were then assembled using HiRise (Putnam *et al.* 2016).

The HiFi+Omni-C assembly was then scaffolded to chromosome-length by the DNA Zoo Consortium following the methodology described here: [www.dnazoo.org/methods](http://www.dnazoo.org/methods). Briefly, in situ Hi-C data from  $\sim 2$  M fibroblasts were generated following the Rao *et al.* (2014) protocol, processed using Juicer (Durand, Shamim, *et al.* 2016), and input into the 3D-DNA pipeline (Dudchenko *et al.* 2017) to produce a candidate chromosome-length genome assembly. We performed additional finishing on the scaffolds using Juicebox Assembly Tools (Durand, Robinson, *et al.* 2016; Dudchenko *et al.* 2018).

We assembled the mitogenome using both the HiFi data and publicly available short-read data (SRR11431899) from the same individual. We assembled mitogenomes from the short-read data using NOVOPlasty (Dierckxsens *et al.* 2020) and GetOrganelle (Jin *et al.* 2020), then mapped HiFi reads

to the consensus using minimap2 (Li 2021), retaining primary reads <16,500-bp, to generate a consensus mitogenome sequence.

We summarized statistics of the assemblies using the `assemblathon_stats.pl` script, and assessed the completeness of the assembly against the `eukaryota_odb10` and `glire_s_odb10` databases using BUSCO, ver 4.0.1 (Simão *et al.* 2015). To estimate the genome size, we quantified k-mers (17–25-mer) from the short-read data using Jellyfish (Marçais and Kingsford 2011) and GenomeScope (Vurture *et al.* 2017).

We evaluated synteny between the PPM genome assembly and the Ord’s kangaroo rat (*D. ordii*) genome (Dord\_2.0) and banner-tailed kangaroo rat (*D. spectabilis*) genome (GCA\_019054845.1). We aligned chromosome-length PPM scaffolds and scaffolds >10 MB for each kangaroo rat using lastz v1.04 (Harris 2007). We compared PPM genome assemblies by liftOver using Flo (<https://github.com/wurmlab/flo>).

### Gene Annotation

Genes were annotated by the NCBI Eukaryotic Genome Annotation Pipeline v. 9.0 (Thibaud-Nissen *et al.* 2013). RNA was extracted from fibroblasts, liver, skeletal muscle, and heart (supplemental table S4, Supplementary Material online). Libraries were generated from 100 ng of total RNA, and 9.96 GB of 75-bp reads were used for gene prediction, along with RNAseq data from kidney

and spleen tissue of four Bailey's pocket mouse (*Chaetodipus baileyi*) samples (SAMN03068786-9), and from five kidney samples of rock pocket mice (*Chaetodipus intermedius*; SAMN15773208-12). The mitochondrial genome was annotated with the MITOS Web server (Bernt *et al.* 2013) and visualized with MitoAnnotator (Iwasaki *et al.* 2013).

### Heterozygosity, ROH, and PSMC Analysis

We estimated variant sites across the genome using the publicly available, paired-end 250 bp read data (SRR11431899). We trimmed adapters, mapped the reads to our assembly, removed read duplicates, and called variants using HaplotypeCaller in GATK v3.8 (Van der Auwera and O'Connor 2020). We estimated heterozygosity in 50–500 KB windows, accounting for sites with missing data using pixy v.1.1 (Korunes and Samuk 2021). To estimate ROH, we summed consecutive 50 KB windows with heterozygosity  $< 0.0002$  (0.2 variants/KB). This threshold was equivalent to the 99th percentile of the heterozygosity distribution on the X chromosome, which is haploid in the male reference individual and thus represents sequencing and mapping error. To prevent long ROH from being spuriously broken, single 50 KB windows with heterozygosity  $< 0.0004$  that had mean heterozygosity  $< 0.0002$  in the surrounding 1 MB were allowed in ROH.

To estimate historical trends in effective population size, we ran 25 replicates of PSMC (Li and Durbin 2011), using settings established for the Norway rat (Deinum *et al.* 2015), a mutation rate of  $2.96 \times 10^{-9}$  and generation time of 1 year.

### Supplementary Material

Supplementary data are available at Genome Biology and Evolution online.

### Acknowledgements

We thank Shauna King, Brigid Moran, Emma Choi, and Anna Sheydina for sample collection and preparation of fibroblast cells for transport. Samples were collected for the Conservation Breeding Program funded by CDFW through the Traditional Section 6 Program and the FWS, and permitted under FWS 10A1A permit number 142435-6 and a CDFW Letter Permit to DMS.

### Funding

This work was supported by Morris Animal Foundation [grant number D19ZO-082 to A.P.W., C.C.S., and D.M.S.]. DNA Zoo Consortium ([www.dnazoo.org](http://www.dnazoo.org)) is supported by Illumina, Inc.; IBM; Pawsey Supercomputing Center; Welch Foundation [grant number Q-1866 to

E.L.A.]; McNair Medical Institute [to E.L.A.]; National Institutes of Health [grant numbers UM1HG009375, RM1HG011016-01A1 to E.L.A.]; US-Israel Binational Science Foundation [grant number 2019276 to E.L.A.]; and National Science Foundation [grant numbers NSF DBI-2021795, NSF PHY-2019745 to E.L.A.]. S.P.T. was supported by National Science Foundation [grant number NSF DEB 1928891].

### Data Availability

The contact matrices are available at [https://www.dnazoo.org/assemblies/Perognathus\\_longimembris\\_pacificus](https://www.dnazoo.org/assemblies/Perognathus_longimembris_pacificus) and <https://tinyurl.com/25vywofz>. The genome assembly has been deposited at DDBJ/ENA/GenBank under the accession JALGBO000000000. Sequence data have been deposited at the NCBI under PRJNA818714. The gene annotation is available as NCBI *Perognathus longimembris pacificus* Annotation Release 100.

### Literature Cited

- Zoonomia Consortium. 2020. A comparative genomics multitool for scientific discovery and conservation. *Nature* 587:240–245.
- Abascal F, et al. 2016. Extreme genomic erosion after recurrent demographic bottlenecks in the highly endangered Iberian lynx. *Genome Biol.* 17:251.
- Armstrong EE, et al. 2021. Recent evolutionary history of tigers highlights contrasting roles of genetic drift and selection. *Mol Biol Evol.* 38:2366–2379.
- Bernt M, et al. 2013. MITOS: improved de novo metazoan mitochondrial genome annotation. *Mol Phylogenet Evol.* 69:313–319.
- Blaxter M, et al. 2022. Why sequence all eukaryotes? *Proc Natl Acad Sci U S A.* 119(4):e2115636118.
- Bolger DT, et al. 1997. Response of rodents to habitat fragmentation in coastal southern California. *Ecol Appl.* 7:552–563.
- Brůna T, Hoff KJ, Lomsadze A, Stanke M, Borodovsky M. 2021. BRAKER2: automatic eukaryotic genome annotation with GeneMark-EP+ and AUGUSTUS supported by a protein database. *NAR Genom Bioinform.* 3:lqaa108.
- Brylski P, Hays L, Avery J. 1998. Recovery plan for the Pacific pocket mouse (*Perognathus longimembris pacificus*). Portland (OR): U.S. Fish and Wildlife Service.
- Ceballos FC, Joshi PK, Clark DW, Ramsay M, Wilson JF. 2018. Runs of homozygosity: windows into population history and trait architecture. *Nat Rev Genet.* 19:220–234.
- Chin C-S, Khalak A. 2019. Human genome assembly in 100 minutes. *bioRxiv.* doi:10.1101/705616.
- Deinum EE, et al. 2015. Recent evolution in *Rattus norvegicus* is shaped by declining effective population size. *Mol Biol Evol.* 32:2547–2558.
- Dierckxsens N, Mardulyn P, Smits G. 2020. Unraveling heteroplasmy patterns with NOVOPlasty. *NAR Genom Bioinform.* 2(1):lqz011.
- Dudchenko O, et al. 2017. De novo assembly of the *Aedes aegypti* genome using Hi-C yields chromosome-length scaffolds. *Science* 356:92–95.
- Dudchenko O, et al. 2018. The Juicebox Assembly Tools module facilitates de novo assembly of mammalian genomes with chromosome-length scaffolds for under \$1000. *bioRxiv.* doi:10.1101/254797.

- Durand NC, Robinson JT, et al. 2016. Juicebox provides a visualization system for Hi-C contact maps with unlimited zoom. *Cell Syst.* 3: 99–101.
- Durand NC, Shamim MS, et al. 2016. Juicer provides a one-click system for analyzing loop-resolution Hi-C experiments. *Cell Syst.* 3:95–98.
- Girgis HZ. 2015. Red: an intelligent, rapid, accurate tool for detecting repeats de-novo on the genomic scale. *BMC Bioinf.* 16:227.
- Hafner JC, et al. 2007. Basal clades and molecular systematics of heteromyid rodents. *J Mammal.* 88:1129–1145.
- Harder AM, Walden KKO, Marra NJ, Willoughby JR. 2022. High-quality reference genome for an arid-adapted mammal, the banner-tailed kangaroo rat (*Dipodomys spectabilis*). *Genome Biol Evol.* 14: evac005.
- Harris RS. 2007. Improved pairwise alignment of genomic DNA [Ph.D. thesis]. State College (PA): The Pennsylvania State University.
- Hedrick PW, Garcia-Dorado A. 2016. Understanding inbreeding depression, purging, and genetic rescue. *Trends Ecol Evol (Amst).* 31:940–952.
- Hu J-Y, et al. 2020. Genomic consequences of population decline in critically endangered pangolins and their demographic histories. *Natl Sci Rev.* 7:798–814.
- Iwasaki W, et al. 2013. Mitofish and MitoAnnotator: a mitochondrial genome database of fish with an accurate and automatic annotation pipeline. *Mol Biol Evol.* 30:2531–2540.
- Jin J-J, et al. 2020. Getorganelle: a fast and versatile toolkit for accurate de novo assembly of organelle genomes. *Genome Biol.* 21:241.
- King SND, et al. 2020. Conservation breeding and reintroduction of the Pacific pocket mouse (*Perognathus longimembris pacificus*), 2019 Annual Report. San Diego Zoo Institute for Conservation Research.
- King SND, et al. 2022. Conservation breeding and reintroduction of the Pacific pocket mouse (*Perognathus longimembris pacificus*), 2021 annual report. San Diego Zoo Wildlife Alliance.
- Korunes KL, Samuk K. 2021. P<sub>LIK</sub>: unbiased estimation of nucleotide diversity and divergence in the presence of missing data. *Mol Ecol Resour.* 21:1359–1368.
- Li H. 2021. New strategies to improve minimap2 alignment accuracy. *Bioinformatics* 37(23):4572–4574.
- Li H, Durbin R. 2011. Inference of human population history from individual whole-genome sequences. *Nature* 475:493–496.
- Liu L, et al. 2021. Genetic consequences of long-term small effective population size in the critically endangered pygmy hog. *Evol Appl.* 14:710–720.
- Marçais G, Kingsford C. 2011. A fast, lock-free approach for efficient parallel counting of occurrences of k-mers. *Bioinformatics* 27: 764–770.
- McKnight ML. 1995. Mitochondrial DNA Phylogeography of *Perognathus amplus* and *Perognathus longimembris* (Rodentia: Heteromyidae): a possible mammalian ring species. *Evolution* 49:816–826.
- McKnight ML, Lee MR. 1992. Karyotypic variation in the pocket mice *Perognathus amplus* and *P. longimembris*. *J Mammal.* 73:625–629.
- Patton JL. 1967. Chromosome studies of certain pocket mice, genus *Perognathus* (Rodentia: heteromyidae). *J Mammal.* 48:27–37.
- Putnam NH, et al. 2016. Chromosome-scale shotgun assembly using an in vitro method for long-range linkage. *Genome Res.* 26:342–350.
- Rao SSP, et al. 2014. A 3D map of the human genome at kilobase resolution reveals principles of chromatin looping. *Cell* 159: 1665–1680.
- Rhie A, et al. 2021. Towards complete and error-free genome assemblies of all vertebrate species. *Nature* 592:737–746.
- Robinson JT, et al. 2018. Juicebox.js provides a cloud-based visualization system for Hi-C data. *Cell Syst.* 6:256–258.e1.
- Robinson JA, et al. 2021. Genome-wide diversity in the California condor tracks its prehistoric abundance and decline. *Curr Biol.* 31: 2939–2946.e5.
- Romanenko SA, Volobouev V. 2012. Non-Sciuriform rodent karyotypes in evolution. *Cytogenet Genome Res.* 137:233–245.
- Schrider DR, Shanku AG, Kern AD. 2016. Effects of linked selective sweeps on demographic inference and model selection. *Genetics* 204(3):1207–1223.
- Shier DM. 2014. Captive breeding, anti-predator behavior and reintroduction of the Pacific pocket mouse (*Perognathus longimembris pacificus*) for the years 2012–2014. San Diego Zoo Institute for Conservation Research.
- Simão FA, Waterhouse RM, Ioannidis P, Kriventseva EV, Zdobnov EM. 2015. BUSCO: assessing genome assembly and annotation completeness with single-copy orthologs. *Bioinformatics* 31:3210–3212.
- Smit AF. 2004. Repeat-Masker Open-3.0. <http://www.repeatmasker.org>.
- Spencer WD. 2005. Recovery research for the endangered Pacific pocket mouse: an overview of collaborative studies. USDA Forest Service General Technical Report.
- Swei A, Brylski PV, Spencer WD, Dodd SC, Patton JL. 2003. Hierarchical genetic structure in fragmented populations of the Little Pocket Mouse (*Perognathus longimembris*) in Southern California. *Conserv Genet.* 4:501–514.
- Thibaud-Nissen F, Souvorov A, Murphy T, DiCuccio M, Kitts P. 2013. Eukaryotic genome annotation pipeline. In: *The NCBI handbook [Internet]*. 2nd ed. Bethesda (MD): National Center for Biotechnology Information.
- Thompson EA. 2013. Identity by descent: variation in meiosis, across genomes, and in populations. *Genetics* 194:301–326.
- Totikov A, et al. 2021. Chromosome-level genome assemblies expand capabilities of genomics for conservation biology. *Genes (Basel)*. 12:1336.
- Van der Auwera GA, O'Connor BD. 2020. Genomics in the cloud: using docker, GATK, and WDL in terra. Sebastopol (CA): O'Reilly Media.
- Vandergast AG, Bohonak AJ, Hathaway SA, Boys J, Fisher RN. 2008. Are hotspots of evolutionary potential adequately protected in southern California? *Biol Conserv.* 141:1648–1664.
- van der Valk T, Díez-Del-Molino D, Marques-Bonet T, Guschanski K, Dalén L. 2019. Historical genomes reveal the genomic consequences of recent population decline in Eastern gorillas. *Curr Biol.* 29:165–170.e6.
- Vurtture GW, et al. 2017. Genomescope: fast reference-free genome profiling from short reads. *Bioinformatics* 33:2202–2204.
- Waser PM, De Woody JA. 2006. Multiple paternity in a philopatric rodent: the interaction of competition and choice. *Behav Ecol.* 17: 971–978.
- Wilder AP, et al. 2020. Fitness costs associated with ancestry to isolated populations of an endangered species. *Conserv Genet.* 21: 589–601.
- Zhou X, et al. 2020. Beaver and naked mole rat genomes reveal common paths to longevity. *Cell Rep.* 32:107949.

Associate editor: David Enard